Two-bubble instabilities in quasi-two-dimensional foams

M.F. VAZ [1] and **S.J. COX** [2]
[1] Instituto de Ciência de Materiais e Superfícies
and Departamento de Engenharia de Materiais,
Instituto Superior Técnico, Av. Rovisco Pais, 1096 Lisboa Codex, Portugal
[2]Institute of Mathematical and Physical Sciences,
University of Wales Aberystwyth, Ceredigion SY23 3BZ, UK.

12th May 2005

Abstract

We study the effect of the experimental set-up on the structure and rheology of two-dimensional foams. We perform the same experiment, in which a sequence of topological instabilities is realized, in three different set-ups, allowing the relative merits of each system to be discussed. The experiment consists of an in-plane deformation of two bubbles which are confined laterally by bars and wholly or partially confined above and below by glass plates and liquid surfaces. An instability of the bubbles occurs when the bar spacing is increased or decreased (traction or compression) beyond a critical value. The critical values depend strongly on the experimental set-up used, and, because of the finite liquid fraction of the system, do not always agree with predictions based upon a two-dimensional analysis of a dry foam. This behaviour gives information about the discrepancies between reported experimental results on macroscopic two-dimensional foams under shear.

1 Introduction

The field of liquid foams has attracted much attention in recent years. Three-dimensional (3D) foams are familiar from daily experience, but are difficult to work with from both an experimental and theoretical point of view. However, two-dimensional (2D) systems allow the determination of several properties of foam that can be extended to 3D. These 2D systems are much easier to analyse; for example, in an experiment, every bubble can be seen and its position and shape monitored. Computer simulations of 2D foams are much faster than their 3D counterparts, and are thus able to be extended to much larger systems, with many thousands of bubbles. We will describe three methods for the experimental production of 2D foams below. By comparing all

three different methods, we show in this paper how the choice of method affects the structure and response of the foam.

Recent interest in the rheology of foams stems from a 2D Couette shear experiment by Debregeas et al. [1]. An aqueous foam was trapped between two horizontal glass plates in an annular cell, and sheared by moving the inner wall in a quasi-static manner (i.e. the strain-rate was low enough that full elastic relaxation could occur between each small increment in strain). The striking result was that all the plastic events (topological changes) were confined to a region close to the inner wall (shear banding). This result was unexpected for a foam in the quasi-static limit. A different Couette shear experiment was carried out by Dennin and co-workers [2, 3, 4] in a cell in which, instead of a glass plate, the foam was bounded below by the surface of a liquid pool, and unbounded above. In this case shear banding was either not observed [2], or the shear band was located much farther from the inner cylinder [3]. Our study is partly motivated by trying to explain this discrepancy between ostensibly similar experiments with different setups.

The work described here also relates to instabilities of foams in apparently 2D systems. Related studies have found that the investigation of topological instabilities is a profitable way to better understand foam systems and to improve the agreement between theoretical predictions and experimental results [5]. The analysis of such instabilities relies on the assumption of the two-dimensionality of the system, considering small plate separations and assuming a low liquid fraction, i.e. the foam to be dry, so that gravity does not play a large role.

Recently, attention has been drawn to the 3D nature of experimental systems. Cox et al. [6] have shown that topological changes predicted by the theory of dry foams may occur at different values in the experimental system because of the unaccounted for liquid, for example in the meniscus beneath the bubbles. Thus experimental configurations are favoured which have higher 2D energies than those configurations predicted by dry theory. The differences between the standard methods of producing 2D bubble clusters suggest different behaviours of the instabilities [7].

The most common methods used to produce 2D foams are (i) a bubble raft, (ii) a Hele-Shaw cell or (iii) a liquid-glass system. These are illustrated in Figure 1. In each experimental system there is a distribution of liquid around the bubbles, which is not accounted for in the standard dry theory. When a soap film touches a glass plate or when three films meet, a small triangular liquid channel, known as a Plateau border, is formed. The liquid in the Plateau borders, and in the menisci where films meet a liquid surface, will cause discrepancies in the response of the experiment, compared to the dry case, which we will quantify. Our experiments thus allow us to begin to explain the difference in the Couette shear experiments referred to above, in which shear banding is seen in a Hele-Shaw geometry but not in a bubble raft.

The bubble raft method was used by Bragg and Nye [8] to reproduce the behaviour of atoms. In this case a single layer of bubbles is created on a liquid surface. Despite the ease of foam creation, this method has the disadvantage of rapid bubble rupture, due to the large region of contact with air. Also, its response cannot always be reconciled with the usual 2D model of foams, in that a topological transition may result in bubbles separating rather than being linked by a common film, as shown below. The liquid content, as measured by the size of the meniscus encompassing the base of each film, is difficult to control.

In the Hele-Shaw or glass/glass method [9], a layer of bubbles is sandwiched between two horizontal glass or perspex plates. Plateau borders are formed at the top and bottom of each film

and along the vertical lines of intersection of the films. The top Plateau border is smaller than the bottom one due to gravity, and the vertical films interpolate between them, in hydrostatic balance. This procedure was first used by Smith [10] and adopted by several authors to study coarsening (bubble growth due to gas diffusion) [e.g. 11]. It is generally the method which allows experiments with the lowest liquid fraction. However, the presence of the glass plates creates difficulties in the manipulation of bubbles, and it is therefore difficult to produce arrangements of bubbles with a given topology.

In the third method, the bubbles are trapped between a glass plate and a liquid solution [12]. In addition to the Plateau borders touching the upper glass plate, as in the glass/glass method, there is a meniscus at the base of each film, as in a bubble raft, which is generally larger than the Plateau border above it. This method was also introduced by Smith [10], although each system was for a different purpose, so that he did not compare the results of the same experiment between the two methods. This glass/liquid method has several advantages: it is easy to produce many topological configurations of bubbles quickly, and to vary the effective liquid fraction of the foam by changing the separation between liquid and glass (large separations correspond to lower liquid fractions). However, in common with the bubble raft, it is difficult to define precisely this liquid fraction, because of the presence of the meniscus, and the meniscus may cause topological changes that are not predicted by dry theory.

In this paper, we make identical experiments on these three systems, shown in Figure 2, choosing a simple experiment to allow us to easily study the effect of the system. The experiments consist of the deformation of two bubbles between two bars, where the distance between the bars is increased (traction) or decreased (compression) to trigger a change in topology, as in the 3D experiments of Bohn [13]. These instabilities occur for critical values of the bar spacing. A small number of experimental results of the two-bubble instabilities prepared with the liquid/glass technique were given by Fortes et al. [14]. Those authors also provided an analytical analysis which we discuss below, although note that in our experiments none of the films are ever pinned to the wall at any point.

The structure of this paper is as follows. In §2 we describe the experiment and the three experimental systems, then give theoretical predictions for the critical bar spacings in §3. In §4 we present the results and discuss them in §5.

2 Experiments

Figure 1 illustrates the three experimental set-ups used to produce 2D foams: a) bubble raft, $\mathcal{LA}$, b) glass/glass, $\mathcal{GG}$ and c) liquid/glass, $\mathcal{LG}$. While in the first method the bubbles are only in contact with the liquid pool ($\mathcal{L}$) and air ($\mathcal{A}$), in the other two methods the bubbles are confined by either the liquid pool and the glass ($\mathcal{G}$), or the two glass plates.

Figure 2(iii) shows two bubbles produced with the liquid/glass method. Two parallel bars penetrate into the liquid solution. One bar is fixed and the other bar moves parallel to the fixed one. A glass plate covers the two bars. Two equal-volume bubbles are produced from a graduated syringe inserted in the liquid, so that their volume V is known. In this way, the bubbles are formed between the surfactant solution and the glass plate covering it at a separation H.

In the bubble raft system, Figure 2(i), the procedure is the same except that we do not cover the bubbles with the glass plate. In the glass/glass system shown in Figure 2(ii), the bottom liquid is replaced by a glass plate, on which the bubbles are formed before covering with a second plate, again at a separation H.

We denote by w the distance between the two bars. The experiment consists of increasing and decreasing the spacing w in small steps (of about 1mm), interspersed with pauses to allow the system to re-equilibrate (i.e. quasi-static motion). We measured the critical values of the spacing at which transitions between various bubble configurations occur.

We made experiments with various separations H (0.5, 1.0 and 1.5 cm) and bubble volumes V (0.5, 1 and 1.5 cm^3).

The bubbles are deformed by changing the distance between the bars w. We start with configuration $\mathcal{P}$ (Figure 3(i)) in which the two bubbles contact each other in a film parallel to the bars. We first increase w (traction) and at a critical bar spacing w_{PN} an instability occurs in which this film disappears and re-forms in the other direction, known as a T1 process. This new configuration, $\mathcal{N}$ (Figure 3(ii)), has a film perpendicular to the bars, joining the two bubbles. In the experimental system $\mathcal{LA}$ this film does not form, and the bubbles separate to form a configuration $\mathcal{N}'$ consisting of two semi-circular bubbles.

We then compress configuration $\mathcal{N}$ by decreasing w and we obtain configuration $\mathcal{P}$ again, at a critical value w_{NP}. Further compression leads to the slant configuration, $\mathcal{S}$ (Figure 3(iii)), without a change of topology, at a value w_{PS}; here the inter-bubble film is inclined, representing a buckling transition. After further compression, the inter-bubble film touches the bars and the bubbles undergo a T1 topological transformation into the bamboo structure $\mathcal{B}$ (Figure 3(iv)), which consists of two bubbles which share a common film perpendicular to the bars. This is attained at a critical value, w_{SB}.

3 Theoretical Predictions

The driving force for the topological changes is the minimization of surface energy. For an idealized two-dimensional foam, the surface energy is equivalent to the line-length, or perimeter, of the configuration. In the dry model of a 2D foam at equilibrium, the films are represented as circular arcs which meet three-fold at 120° in vertices, according to Plateau's rules [15]. It is then possible to calculate geometrically an idealized 2D energy for each of the bubble configurations considered here, shown in Table 1.

The decoration of this structure with a triangular Plateau border at each vertex, representing the vertical Plateau borders in the experiments, is the most easily achieved representation of a wet 2D foam. In practice, the main effect of the Plateau borders is to change the vertex separation at which T1s occur. Such a model does not, however, take into account any variation of Plateau border area with height.

We give here two predictions for the bar-spacing at which the topological changes occur. The first is based upon the usual dry model of a 2D foam, the second on an effectively "wet" 2D foam.

Our first theoretical prediction of the critical bar-spacing arises by calculating the value of w at which a soap film shrinks to zero length, as in the idealized dry model of a 2D foam. At this point,

	$E(A,w)$	$L(A,w)$
P	$\frac{2A}{w} + w\left(\frac{\sqrt{3}}{2} + \frac{\pi}{3}\right)$	$\frac{2A}{w} - \frac{w}{2}\left(\frac{2\pi}{3} - \sqrt{3}\right)$
N	$w + \left(\frac{4\pi}{3\sqrt{3}-1} - 1\right)\sqrt{\frac{36A}{4\pi - 3\sqrt{3}}}$	$\frac{w}{2} - \sqrt{\frac{A}{4\pi - 3\sqrt{3}}}$
N'	$2\sqrt{2\pi A}$	$w - 2\sqrt{\frac{A}{\pi}}^{\dagger}$
S	$2\sqrt{2A\left(\frac{\sqrt{3}}{2} + \frac{\pi}{3}\right)}$	$\frac{w}{\cos\alpha}\left(\frac{\pi}{6} - \alpha\right)^{\ddagger}$
B	$3w$	$-$

Table 1: The 2D energy (line-length) and the length of the film that shrinks to zero length to trigger the T1, as a function of bubble area A and bar spacing w. † the distance between the two separated semicircles. ‡ $\cos(\alpha) = \sqrt{\frac{w}{2A}\left(\frac{\sqrt{3}}{2} + \frac{\pi}{3}\right)}$.

two vertices touch and trigger a topological change. The lengths L of these films are given in the last column of Table 1 for 2D bubbles of area A. They are calculated directly from the geometry of the cluster, as demonstrated by Fortes et al. [14]: for the transition $\mathcal{S}$ to $\mathcal{B}$ they predict a value of $w_{SB} = 0.885\sqrt{A}$, which is the point at which one of the short films touching the bar disappears. The other values are $w_{PN} = 3.322\sqrt{A}$, when the common film shrinks to zero length in the $\mathcal{P}$ configuration; $w_{NP} = 2.210\sqrt{A}$, when the film joining the bubbles in the $\mathcal{N}$ configuration shrinks to zero length; and $w_{N'P} = 1.128\sqrt{A}$, when the two semi-circular bubbles touch. These values are reduced, in proportion to the square-root of the liquid fraction, as the foam becomes wetter, since the vertices touch sooner.

The transition from $\mathcal{P}$ to $\mathcal{S}$ does not involve a topological change: the change to the alternative configuration should occur when it is energetically favourable to do so. By comparing the energy E of each configuration (lines 1 and 4 of Table 1), Fortes et al. [14] predicted that the value of w at which the $\mathcal{P}$ to $\mathcal{S}$ transition occurs is $w_{PS} = 1.022\sqrt{A}$.

The energetic analysis given above is also applicable to a foam that does not have vanishingly small liquid fraction [6]. The effect of the excess liquid is to allow the bubbles to jump to an alternative configuration as soon as the energy of this alternative configuration, measured for the equivalent (undecorated) dry foam, is lower. Our second prediction, for wet foams, is that the critical spacing w_{ij} is the value of w for which the energy of configuration i is equal to the energy of configuration j. These values are $w_{PN} = 2.586\sqrt{A}$, $w_{PN'} = 2.129\sqrt{A}$ and $w_{SB} = 1.304\sqrt{A}$.

These should be considered as upper and lower bounds, because of the effects of liquid content. The first prediction, of films shrinking to zero length, should provide an upper bound for the critical spacing at which the transition occurs in traction ($\mathcal{P} - \mathcal{N}$) and a lower bound in compression. Similarly, the second prediction should give lower and upper bounds in traction or compression respectively.

4 Results

In Figure 4 we plot the critical values of w as a function of bubble volume V for the transitions $\mathcal{P}-\mathcal{N}'$, $\mathcal{N}'-\mathcal{P}$, $\mathcal{P}-\mathcal{S}$ and $\mathcal{S}-\mathcal{B}$, obtained with the bubble raft experiment, $\mathcal{LA}$. The results are scaled by an equivalent cross-sectional area that assumes that the bubbles are hemispherical, $A_s = \pi(3V/(2\pi))^{2/3}$. That the results do not change for different bubble volumes suggests that this scaling is appropriate, and that for the other systems we need only concentrate on the variation of w with plate separation H.

In traction, the $\mathcal{P}-\mathcal{N}'$ transition occurs as soon as it is energetically favourable to do so, in good agreement with the second analytic prediction for "wet" foams. This reflects the (uncontrollable) wetness of this experimental system, which induces the transition. In compression, there is a slight delay after the energies become equal before the $\mathcal{N}'$ configuration of two separated bubbles rejoins to form $\mathcal{P}$, but it still occurs before the idealized picture of two semi-circles that just touch suggests it should (first theoretical prediction). It represents, in fact, the extent of the meniscus, and the distance at which two bubbles start to be attracted to each other [16]. The $\mathcal{S}$ configuration appears where predicted, but the transition from $\mathcal{S}$ to $\mathcal{B}$ does not occur until the edge length shrinks to zero, as in a dry foam. Apart from this last discrepancy, we expect that the wet predictions will be most useful for the $\mathcal{LA}$ system.

In the experiments where the foam is covered by a glass plate, shown in Figure 5, the values of the spacing w are scaled by the square-root of the apparent area of each bubble, $A = V/H$, where H took a range of values up to 1.5cm. As the plate separation increases, the effective liquid fraction of the $\mathcal{LG}$ system decreases, while that of the glass/glass system doesn't. Therefore the observation that the critical values of w do not change with H for $\mathcal{GG}$ makes sense. Moreover, all the $\mathcal{GG}$ results are consistent with the predictions of dry 2D theory (solid lines).

The results for the liquid/glass system in traction ($\mathcal{P}-\mathcal{N}$) show that this transition occurs as soon as it is energetically favourable to do so for low separations (relatively high liquid fraction). The values drift towards the other prediction, of waiting for the shortest film to shrink to zero length, as H increases. In compression, the trend of increasing critical w with increasing H is also clear. As H decreases and the system gets wetter, the critical w is smaller and below the lower bound of the second analytic prediction, suggesting that for the $\mathcal{LG}$ system the dry theory is inappropriate.

5 Discussion

The two-dimensional model of an idealized dry foam is an attractive one for theory and computation. It has also been widely invoked as an experimental technique, often without noting the significant defect that no experimental system of this kind is completely two-dimensional (unlike, for example, a Langmuir foam [17, 18], consisting of coexisting gas and liquid phases in a monolayer of amphiphilic molecules on a liquid surface).

Therefore, the disagreement between theoretical and experimental values are due to the 3D nature of the experiments. Both the bubble raft and the liquid/glass methods suffer from the presence of a meniscus around the bubbles, while the confinement in the glass/glass system makes it

awkward to manipulate the bubbles.

It is the glass/glass system, or Hele-Shaw cell, that we have demonstrated to correspond most closely to the dry theory. At the other extreme, the bubble raft is simple to use but bears the least resemblance to the predictions of dry theory, being better approximated by our "wet" theory. Between these two extremes, the glass/liquid system allows the liquid fraction to be controlled: our experiments suggest that it is necessary to take $H/\sqrt{A} < 1$ to be close to the dry limit, and $H/\sqrt{A} > 2$ for our second set of "wet" predictions to be valid.

It should therefore be no surprise if the localization results of the 2D Couette shear experiments of Debregeas et al. [1], performed in the glass/glass system, are found to be in agreement with quasi-static 2D simulations of dry foams in this geometry. More difficult will be a numerical confirmation that the shear-band is not always present [2], or changes position [3], in the bubble raft. The greater liquid content in the latter system surely plays a role in determining the presence of localization.

Such a simulation with the Surface Evolver would require each film to be deleted at least once in each iteration to test whether the energy of an alternative configuration is lower. An alternative would be a full three-dimensional Evolver calculation of a wet foam, which is currently not viable because of the computational time required.

To improve agreement between simulations and experiments on 2D foams, the finite time-scale of a T1 event must be accounted for (T1s occur instantaneously in quasi-static simulations), as in Durian's bubble model [19] for wet foams. Twardos and Dennin [20] have recently shown that for the $\mathcal{LA}$ system, this time-scale is of the order of 10 seconds, a far from insignificant length of time. The same time-scale may not apply to the other two systems: does the presence of a glass plate increase or decrease it? That is, to what extent is this time-scale set by the underlying liquid, or the drag of the Plateau borders on the glass plates, or inter-bubble dissipation?

In our experiments, we find time-scales close to two seconds for the relaxation to equilibrium after the $\mathcal{P} - \mathcal{N}$ change (data not shown) for all systems. This shorter time could be indicative of a change in solution viscosity or the ease with which a foam of two bubbles can relax, in comparison to a bulk foam; it will be investigated in future work.

References

[1] G. Debregeas, H. Tabuteau and J.M. di Meglio. 2001 Deformation and flow of a two-dimensional foam under continuous shear. *Phys. Rev. Lett.* **87**:178305.

[2] J. Lauridsen, M. Twardos and M. Dennin. 2002 Shear-induced stress relaxation in a two-dimensional wet foam. *Phys. Rev. Lett.* **89**:098303.

[3] J. Lauridsen, G. Chanan and M. Dennin. 2004 Velocity profiles in slowly sheared bubble rafts. *Phys. Rev. Lett.* **93**:018303.

[4] M. Dennin. 2004 Statistics of bubble rearrangements in a slowly sheared two-dimensional foam. *Phys. Rev. E* **70**:041406.

[5] D. Weaire, S.J. Cox and F. Graner. 2002 Uniqueness, Stability and Hessian eigenvalues for two-dimensional foam structures. *Eur. Phys. J. E* **7**:123–127.

[6] S.J. Cox, M.F. Vaz and D. Weaire. 2003 Topological changes in a two-dimensional foam cluster. *Eur. Phys. J. E* **11**:29–35.

[7] M.F. Vaz, S.J. Cox and M.D. Alonso. 2004 Minimum energy configurations of small bidisperse bubble clusters. *J. Phys.: Condens. Matter* **16**:4165–4175.

[8] L. Bragg and J.F. Nye. 1947 A dynamical model of a crystal structure. *Proc. R. Soc. Lond.* A**190**:474–481.

[9] H.S. Hele-Shaw. 1898 The Flow of Water. *Nature* **58**:34–36.

[10] C.S. Smith 1952 Grain shapes and other metallurgical applications of topology. In *Metal Interfaces*. American Society for Metals, Cleveland, OH. pp. 65–108.

[11] J.A. Glazier, S.P. Gross and J. Stavans. 1987 Dynamics of two-dimensional soap froths. *Phys. Rev. A* **36**:306–312.

[12] M.F. Vaz and M.A. Fortes. 1997 Experiments on defect spreading in hexagonal foams. *J. Phys.: Condens. Matt.* **9**:8921–8935.

[13] S. Bohn. 2003 Bubbles under stress. *Eur. Phys. J. E* **11**:177–189.

[14] M.A. Fortes, M.E. Rosa, M.F. Vaz and P.I.C. Teixeira. 2004 Mechanical instabilities of bubble clusters between parallel walls. *Euro. Phys. J. E* **15**:395–406.

[15] J.A.F. Plateau. 1873 *Statique Expérimentale et Théorique des Liquides Soumis aux Seules Forces Moléculaires*. Gauthier-Villars, Paris.

[16] M.M. Nicolson. 1949 The Interaction between Floating Particles. *Proc. Camb. Phil. Soc. Math. Phys. Sci.* **45**:288–295.

[17] M. Dennin and C.M. Knobler. 1997 Experimental studies of bubble dynamics in a slowly driven monolayer foam. *Phys. Rev. Lett.* **78**:2485–2488.

[18] S. Courty, B. Dollet, F. Elias, P. Heinig and F. Graner. 2003 Two-dimensional shear modulus of a Langmuir foam. *Europhys. Lett.* **64**:709–715.

[19] D.J. Durian. 1995 Foam Mechanics at the Bubble Scale. *Phys. Rev. Lett.* **75**:4780–4783.

[20] M. Twardos and M. Dennin. 2005 Comparison between step strains and slow steady shear in a bubble raft. *Phys. Rev. E* **71**:061401.

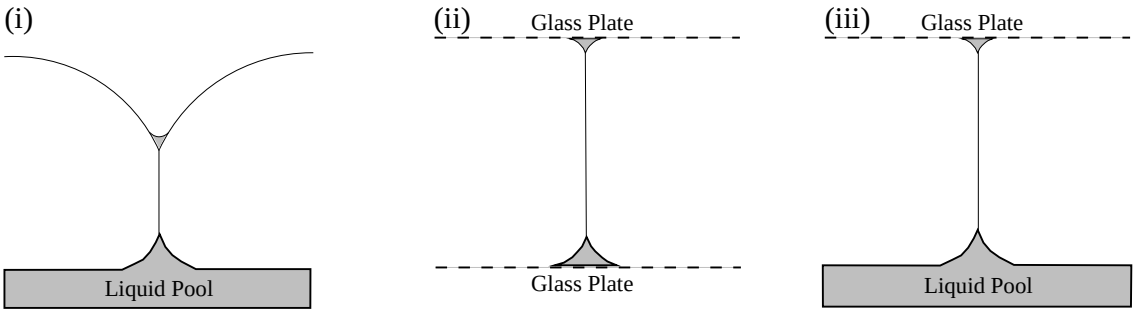

Figure 1: Different quasi-2D experimental set-ups for investigating foams, illustrated in cross-section. (i) a bubble raft, denoted here by $\mathcal{LA}$, in which the bubbles float freely on the surface of a liquid. (ii) $\mathcal{GG}$. (iii) $\mathcal{LG}$. Based upon figure 6 of [6].

(i)

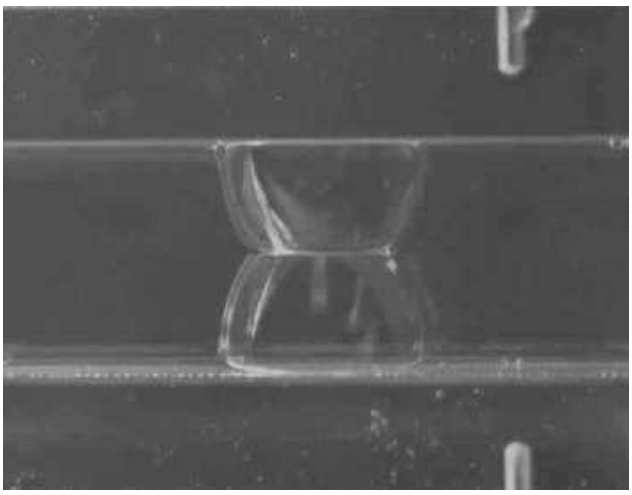

(ii)

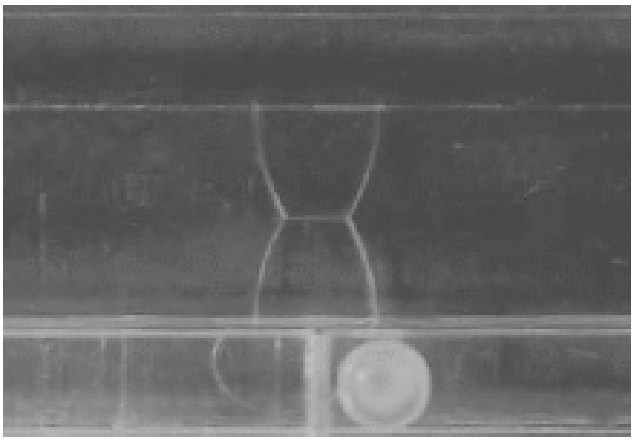

(iii)

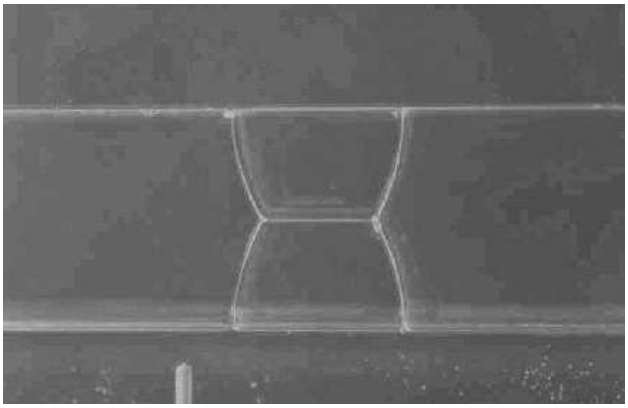

Figure 2: Three experimental systems used to produce 2D foams (top view): (i) bubble raft, $\mathcal{LA}$, (ii) glass/glass, $\mathcal{GG}$ and (iii) glass/liquid, LG. The bar-spacing in each case is of the order of 2cm.

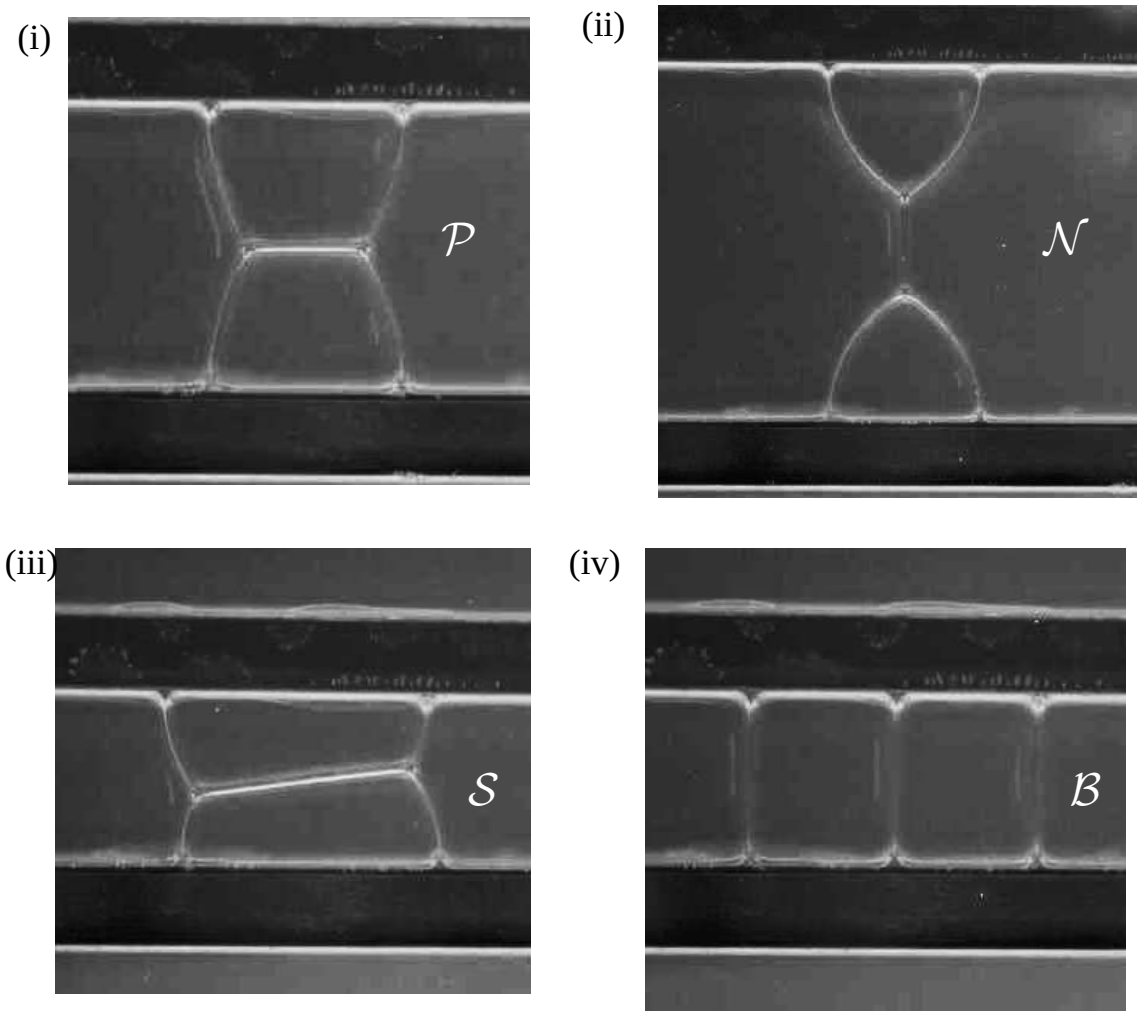

Figure 3: Experimental observations of configurations: (i) $\mathcal{P}$; (ii) $\mathcal{N}$; (iii) $\mathcal{S}$ and (iv) $\mathcal{B}$. The bars are visible at the top and bottom of each image.

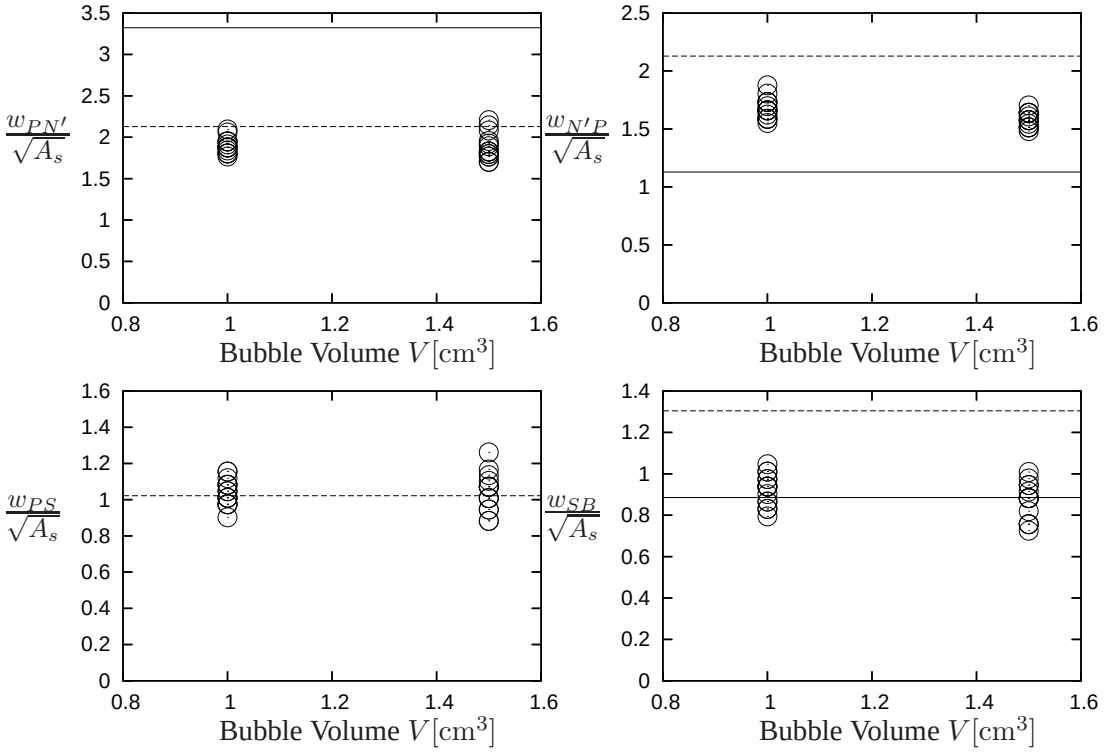

Figure 4: The critical bar spacing as a function of bubble volume V at which the configuration changes for the $\mathcal{LA}$ system, in which the bubbles completely separate in the $\mathcal{P}-\mathcal{N}'$ transition and the "height" of the system does not play any role. In each experiment w is scaled by $\sqrt{A_s}$, where A_s is the area of the base of a hemi-sphere of volume V. The dashed lines represent the critical w from the second analytic prediction (equal energy structures) while the solid lines are the critical w for the first prediction (edge shrinking to zero length). It is clear that varying the bubble volume makes little difference to the results scaled in this way. See text for discussion.

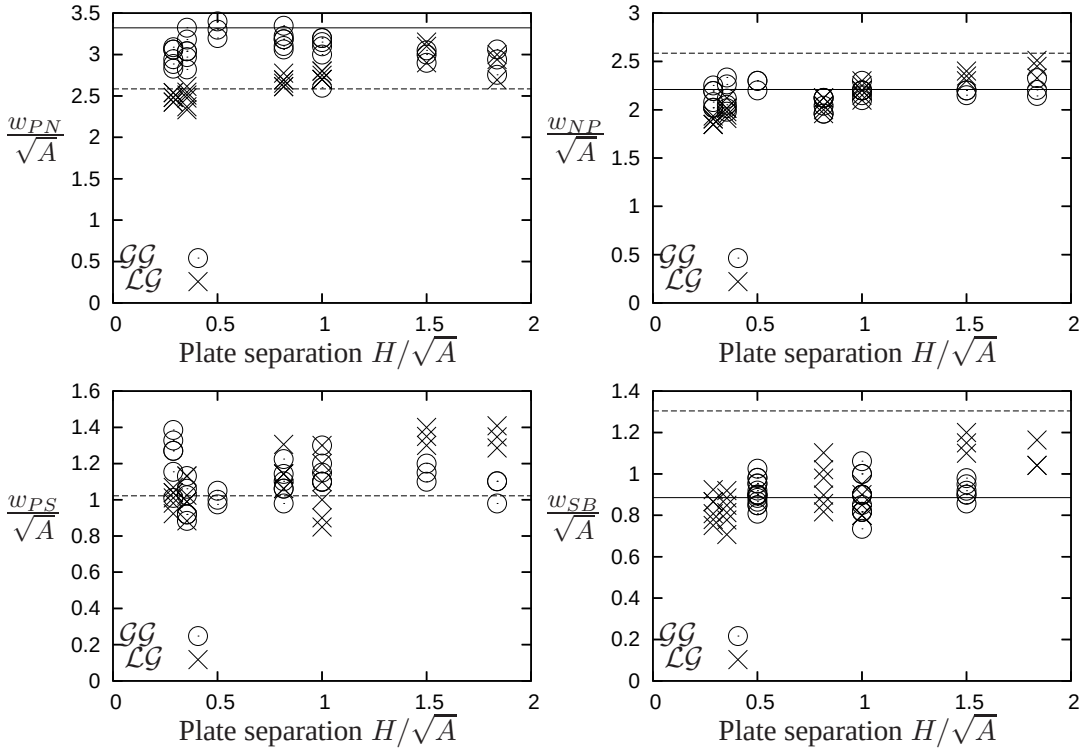

Figure 5: The critical bar spacing as a function of scaled plate separation $H/\sqrt{A}$ at which the configuration changes for the two systems $\mathcal{GG}$ and $\mathcal{LG}$. The dashed lines represent the critical w from the second analytic prediction (equal energy structures) while the solid lines are the critical w for the first prediction (edge shrinking to zero length).